

## Magnetic Properties of an Octanuclear Iron(III) Cation

C. Delfs,<sup>†</sup> D. Gatteschi,<sup>\*†</sup> L. Pardi,<sup>†</sup> R. Sessoli,<sup>†</sup> K. Wieghardt,<sup>\*‡</sup> and D. Hanke<sup>†</sup>

Department of Chemistry, University of Florence, Florence, Italy, and Lehrstuhl für Anorganische Chemie I, Ruhr-Universität, D-4630 Bochum, Germany

Received February 10, 1993

The magnetic properties of  $\{[(\text{tacn})_6\text{Fe}_8(\mu_3\text{-O})_2(\mu_2\text{-OH})_{12}]\text{Br}_7(\text{H}_2\text{O})\}\text{Br}\cdot\text{H}_2\text{O}$ ,  $\text{Fe}_8$ ,  $\text{tacn} = 1,4,7$ -triazacyclononane, a molecule comprising eight iron(III) ions bridged by oxo and hydroxo groups, are reported. The magnetic susceptibility, both dc and ac, and the magnetization indicate that at low-temperature spin levels with  $8 < S < 10$  are populated. EPR confirms that levels of high spin multiplicity are populated at 4.2 K. For the first time an attempt is made to calculate the energy of the spin levels of such a large cluster within a spin Hamiltonian formalism. The 1 679 616 states originating from the coupling of eight  $S = 5/2$  spins are classified by using total spin and point group symmetry, and the Hamiltonian matrix is calculated using an irreducible tensor operator approach. In this way the susceptibility can be calculated, and satisfactory fits of the experimental magnetic susceptibility are achieved. The values of the required parameters compare well with those previously reported in analogous iron complexes.

## Introduction

Polynuclear iron(III) complexes are the focus of very active research aiming at developing synthetic strategies to obtain larger and larger clusters.<sup>1–9</sup> One of the reasons for the interest in these types of materials is that of understanding the properties of ferritin, the iron storage protein of bacteria, plants, and animals, which can store up to 4500 iron atoms as octahedral iron(III) ions connected by oxo bridges.<sup>10,11</sup> One of the features of these large clusters is that of being superparamagnetic,<sup>10,12</sup> due to the dimensions which are intermediate between those of simple paramagnets and those of bulk materials, containing infinite assemblies of interacting centers. This gives an additional reason of interest for the synthesis of large iron and, in general, metal ion clusters, i.e. that of synthesizing magnetic materials of mesoscopic scale, where interesting new properties can be anticipated and where bulk behavior may coexist with paramagnetic properties.<sup>13</sup>

The interpretation of the magnetic properties of large metal ion clusters is hampered by the difficulties associated with the calculation of the thermally accessible energy levels and of the thermodynamic properties in systems which are too large to use the simple approaches required for the interpretation of di- and trinuclear clusters but do not afford the simplification associated with translational symmetry of infinite assemblies of spins. In fact up to now only clusters comprising four iron(III) ions<sup>14</sup> have

been successfully tackled in the general case, even if treatments are available for particularly simple larger clusters.<sup>15</sup>

Very recently we have developed in Florence a fast and efficient procedure for the calculation of the spin levels of high-nuclearity spin clusters using irreducible tensor operators,<sup>16</sup> ITO, which we have successfully applied to  $\text{Fe}^{\text{III}}_6$  clusters.<sup>17</sup>

This approach made it possible for the first time to attempt quantitative interpretation of the magnetic properties of high-nuclearity spin clusters: for instance satisfactory fits of the magnetic susceptibility of clusters containing 14 and 15 oxovanadium(IV) ions were obtained.<sup>13</sup>

Recently one of us reported a cluster containing eight high-spin iron(III) ions, of formula  $\{[(\text{tacn})_6\text{Fe}_8(\mu_3\text{-O})_2(\mu_2\text{-OH})_{12}]\text{Br}_7(\text{H}_2\text{O})\}\text{Br}\cdot\text{H}_2\text{O}$ ,  $\text{Fe}_8$ ,  $\text{tacn} = 1,4,7$ -triazacyclononane,<sup>3</sup> whose structure is sketched in Figure 1, but only preliminary magnetic data were reported. We felt that this compound might provide an ideal testing ground for the ITO method to calculate the magnetic susceptibility of large clusters, and we wish to report here its magnetic properties, together with a detailed interpretation based on the extensive use of symmetry in order to reduce the dimensions of matrices. We feel that this represents a case history which can be used as a general model for the interpretation of the magnetic properties of high-nuclearity spin clusters.

## Experimental Section

The compound was prepared as previously described.<sup>3</sup> The static magnetic susceptibility of a powder sample was measured by using a Metronique Ingénierie MS02 SQUID magnetometer. The ac susceptibility of a powder sample was measured on a laboratory-assembled susceptometer based on a mutual inductance bridge at the frequency of 100 Hz. Isothermal magnetization was measured up to 20 T using a Bitter magnet.<sup>18</sup>

## Results

The temperature dependence of  $\chi T$  of  $\text{Fe}_8$  in a field of 2 T is shown in Figure 2. At room temperature  $\chi T$  is 20.06 emu mol<sup>-1</sup> K, much smaller than expected for eight uncoupled  $S = 5/2$  spins, and steadily increases on decreasing temperature, reaching a maximum corresponding to  $\chi T = 45.8$  emu mol<sup>-1</sup> K, at ca 25 K. Below 10 K  $\chi T$  rapidly decreases on decreasing temperature

<sup>†</sup> University of Florence.<sup>‡</sup> Ruhr Universität.

- Gorun, S. M.; Lippard, S. J. *Nature* **1986**, *319*, 666.
- Taft, K. L.; Lippard, S. J. *J. Am. Chem. Soc.* **1990**, *112*, 9629.
- Wieghardt, K.; Pohl, K.; Jibril, I.; Huttner, G. *Angew. Chem., Int. Ed. Engl.* **1984**, *24*, 77.
- McCusker, J. K.; Christmas, C. A.; Hagen, P. M.; Chadha, R. K.; Harvey, D. F.; Hendrickson, D. N. *J. Am. Chem. Soc.* **1991**, *113*, 6114.
- Hegetschweiler, K.; Schmalte, H.; Streit, H. M.; Schneider, W. *Inorg. Chem.* **1990**, *29*, 3625.
- Lippard, S. J. *Angew. Chem., Int. Ed. Engl.* **1988**, *100*, 353.
- Micklitz, W.; Lippard, S. J. *J. Am. Chem. Soc.* **1989**, *111*, 6856.
- Heath, S. L.; Powell, A. K. *Angew. Chem., Int. Ed. Engl.* **1992**, *31*, 191.
- Hagen, K. S. *Angew. Chem., Int. Ed. Engl.* **1992**, *31*, 1010.
- Harrison, P. M.; Artymink, P. J.; Ford, G. C.; Lawson, D. M.; Smith, J. M. A.; Treffry, A.; White, J. L. In *Biominingeralization-Chemical and Biochemical Perspectives*, Mann, S., Webb, J., Williams, R. J. P., Eds.; VCH: Weinheim, Germany, 1989.
- Lippard, S. J. *Chem. Brit.* **1986**, *22*, 222.
- Linderth, S.; Khanna, S. N. *J. Magn. Magn. Mater.* **1992**, *104*, 1574.
- Barra, A. L.; Gatteschi, D.; Pardi, L.; Müller, A.; Döring, J. *J. Am. Chem. Soc.* **1992**, *114*, 8509.
- McCusker, J. K.; Vincent, J. B.; Schmitt, E. A.; Mino, M. L.; Shin, K.; Coggin, D. K.; Hagen, P. M.; Huffmann, J. C.; Christou, G.; Hendrickson, D. N. *J. Am. Chem. Soc.* **1991**, *113*, 3012.

- Christmas, C.; Vincent, J. B.; Chang, H.-R.; Huffman, J. C.; Christou, G.; Hendrickson, D. N. *J. Am. Chem. Soc.* **1988**, *110*, 823.
- Gatteschi, D.; Pardi, L. *Gazz. Chim. Ital.*, in press.
- Gatteschi, D.; Pardi, L. In *Research Frontiers in Magnetochemistry*; O'Connor, C. J., Ed.; World Scientific: Singapore, in press.
- Picoche, J. C.; Guillot, M.; Marchaud, A. *Physica* **1989**, *B155*, 407.

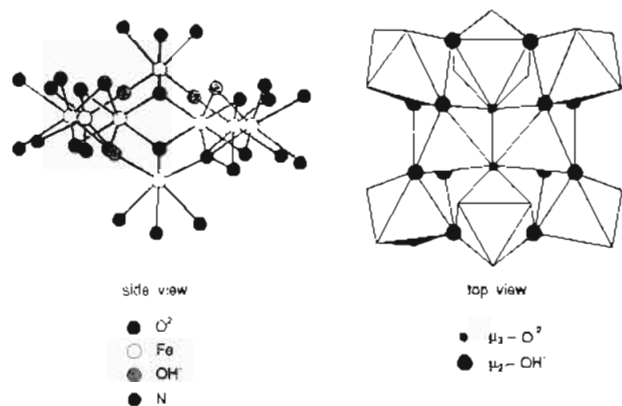


Figure 1. Molecular structure of  $\{[(\text{tacn})_6\text{Fe}_8(\mu_3\text{-O})_2(\mu_2\text{-OH})_{12}]\text{Br}_7(\text{H}_2\text{O})\}\text{Br}\cdot\text{H}_2\text{O}$ ,  $\text{Fe}_8$ .

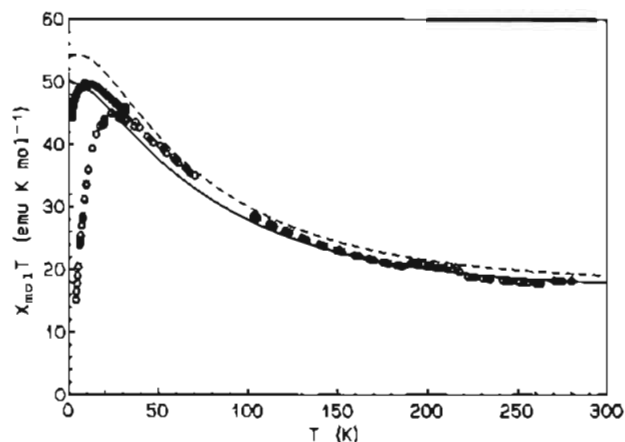


Figure 2. Magnetic Properties of  $\text{Fe}_8$  in the form of  $\chi T$  product vs  $T$ : (O)  $H = 2 \text{ T}$ ; (●)  $H \sim 0$ . Curves represent calculated values of  $\chi T$  for (dashed)  $J_1 = 20$ ,  $J_2 = 120$ ,  $J_3 = 15$ ,  $J_4 = 35 \text{ cm}^{-1}$ , (solid)  $J_1 = 102$ ,  $J_2 = 120$ ,  $J_3 = 15$ ,  $J_4 = 35 \text{ cm}^{-1}$ .

reaching  $15 \text{ emu mol}^{-1} \text{ K}$  at ca.  $2 \text{ K}$ . In order to rule out any effect associated with the presence of an external magnetic field, the measurements were performed also with an ac susceptometer without any applied field. The results drawn as filled circles in Figure 2 indicate that the maximum is higher for the zero-field measurement reaching  $52 \text{ emu mol}^{-1} \text{ K}$  at  $10 \text{ K}$  and that the decrease at lower temperatures is much less marked reaching  $45 \text{ emu mol}^{-1} \text{ K}$  at  $4 \text{ K}$ , suggesting that effects due to saturation affect the measurements at  $H = 2 \text{ T}$ . It is interesting to note that no out of phase response was observed in this case in contrast with the results observed<sup>19</sup> in a  $\text{Mn}_{12}$  cluster, which also has a similar large  $\chi T$  value at low temperature.

In order to determine the field dependence of the magnetization, measurements were performed at  $1.8$  and  $4.2 \text{ K}$ , and the results are shown in Figure 3. The data points at the two temperatures are very close to each other, much closer than expected for an isolated spin multiplet. For both the temperatures and magnetization regularly increases with increasing field and saturates at the value of ca.  $19 \mu_B$  in a field of  $10 \text{ T}$ .

Polycrystalline powder EPR spectra of  $\text{Fe}_8$  were recorded at X-band frequency in the range  $4.2\text{--}300 \text{ K}$  and are shown in Figure 4. At high temperature only a very broad featureless band is observed at  $g \sim 2$ . On cooling some structure starts to appear and eventually at  $4.2 \text{ K}$  at least seven relatively intense transitions are observed. Although they are not exactly equispaced, they are separated by intervals of ca.  $1000 \text{ G}$ . Attempts were made also to record single-crystal spectra, but the obtained crystals were found to be too small to give detectable signals.

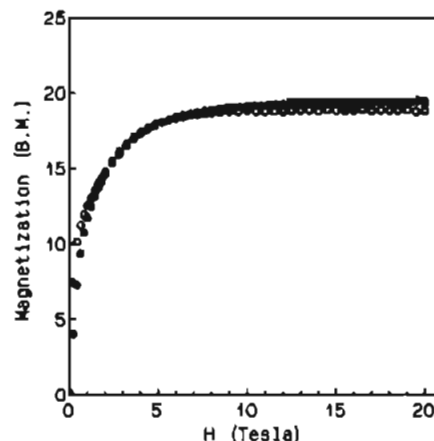


Figure 3. Magnetization curves for  $\text{Fe}_8$ : (●)  $T = 4.2 \text{ K}$ ; (○)  $T = 1.8 \text{ K}$ .

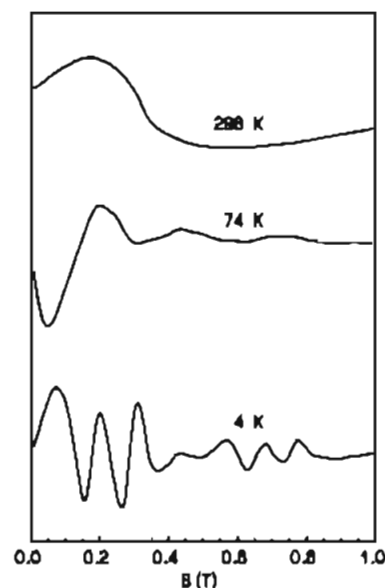


Figure 4. Polycrystalline powder X-band EPR spectra of  $\text{Fe}_8$ .

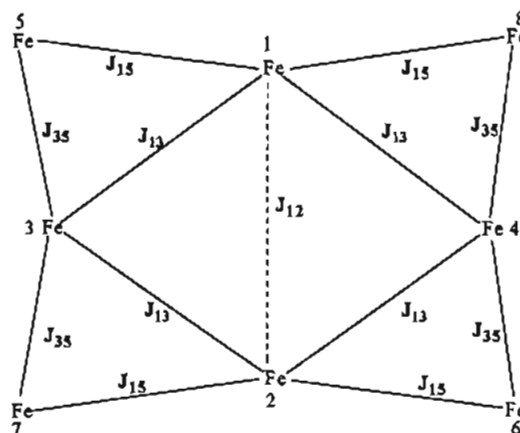


Figure 5. Scheme of the exchange pathways connecting iron(III) centers in  $\text{Fe}_8$ .

## Discussion

**Qualitative Aspects.** The exchange pathways connecting the eight iron(III) ions can be schematized as shown in Figure 5. The four iron(III) ions connected by  $\mu_3$ -oxo bridges have the now well-known "butterfly" configuration, which has been extensively discussed for both iron<sup>14,20,21</sup> and manganese<sup>22,23</sup> tetranuclear

(19) Caneschi, A.; Gatteschi, D.; Sessoli, R.; Barra, A. L.; Brunel, L. C.; Guillot, M. *J. Am. Chem. Soc.* **1991**, *113*, 5873.

(20) Gorun, S. M.; Lippard, S. J. *Inorg. Chem.* **1988**, *27*, 149.

Table I. Group Theoretical Classification of Total Spin States for a Cluster of Four  $S = 5/2$  Spins

$S$	representations in $T_d$	$D_2(S_A)$	$D_2(S_B)$
10	$A_1$	A	A
9	$T_2$	$B_1 + B_2 + B_3$	$A + B_2 + B_3$
8	$A_1 + E + T_2$	$3A + B_1 + B_2 + B_3$	$3A + B_1 + B_2 + B_3$
7	$A_1 + T_1 + 2T_2$	$A + 3B_1 + 3B_2 + 3B_3$	$3A + B_1 + 3B_2 + 3B_3$
6	$2A_1 + 2E + T_1 + 2T_2$	$6A + 3B_1 + 3B_2 + 3B_3$	$6A + 3B_1 + 3B_2 + 3B_3$
5	$A_1 + E + 2T_1 + 4T_2$	$3A + 6B_1 + 6B_2 + 6B_3$	$6A + 3B_1 + 6B_2 + 6B_3$
4	$2A_1 + A_2 + 3E + 2T_1 + 3T_2$	$9A + 5B_1 + 5B_2 + 5B_3$	$8A + 6B_1 + 5B_2 + 5B_3$
3	$A_1 + E + 3T_1 + 4T_2$	$3A + 7B_1 + 7B_2 + 7B_3$	$6A + 4B_1 + 7B_2 + 7B_3$
2	$2A_1 + 3E + A_2 + 2T_1 + 2T_2$	$9A + 4B_1 + 4B_2 + 4B_3$	$7A + 6B_1 + 4B_2 + 4B_3$
1	$2T_1 + 3T_2$	$5B_1 + 5B_2 + 5B_3$	$3A + 2B_1 + 5B_2 + 5B_3$
0	$A_1 + A_2 + 2E$	6A	$3A + 3B_1$

complexes. The butterfly is connected to four other iron ions through hydroxo bridges.  $J_1$  corresponds to the exchange interaction transmitted along the body of the butterfly,  $J_2$  to that transmitted between the body and the wings,  $J_3$  to a di- $\mu_2$ -hydroxo, and  $J_4$  to a single  $\mu_2$ -hydroxo bridge. All these pathways are expected to be antiferromagnetic.<sup>4,14,21</sup> In the butterfly complexes  $J_1$  has been found<sup>14,20</sup> in the range 18–25 cm<sup>-1</sup> and  $J_2$  in the range 90–120 cm<sup>-1</sup>,<sup>14</sup> and the hydroxo bridges have been observed<sup>24</sup> to correspond to interactions in the range 15–35 cm<sup>-1</sup>.

Qualitative conclusions about the nature of the ground state are very difficult to draw, due to the presence of many triangles in the network of interactions, which provide frustration effects when the couplings are all antiferromagnetic as expected in this case. In fact, in a triangle a spin is subject to two conflicting opposite interactions, and as a result the most stable configuration of the spins does not correspond to alignment to either 0 to 180° but to a different angle which depends on the ratio of the conflicting coupling constants.

Particularly large frustration effects have been observed in the butterfly complexes containing manganese,<sup>23</sup> while for the analogous tetranuclear iron complexes the ground state has always been found to be diamagnetic.<sup>14,20</sup> This has been justified with a model where  $J_2$  is much larger than  $J_1$ .<sup>14</sup>

A qualitative analysis of the temperature dependence of  $\chi T$  indicates the presence of antiferromagnetic couplings, because the high-temperature value is much smaller than expected for 8 uncoupled spins. The increase of  $\chi T$  on decreasing temperature indicates that below room temperature low-spin states are selectively depopulated. This is in agreement with frustration effects<sup>4</sup> and with previous findings in large spin clusters.<sup>25</sup> The value of the maximum in  $\chi T$  is intermediate between the values expected for a ground  $S = 9$  (45 emu mol<sup>-1</sup> K) and an  $S = 10$  state (55 emu mol<sup>-1</sup> K). This must be taken as an indication that at ca. 10 K levels with  $S > 8$  are populated.

The saturation value of the magnetization of 19.5  $\mu_B$  at 4.2 K and 18.9  $\mu_B$  at 1.8 K agrees with an  $S = 10$  ground state, even though the fact that the experimental curves at the two different temperatures are almost superimposable and do not follow a Brillouin function for a pure  $S = 10$  state indicates that in this range of temperatures there is not one isolated spin multiplet populated. The best explanation is that a strong field stabilizes the  $S = 10$  state, which is close in energy to an  $S = 9$  state.

The decrease in  $\chi T$  below 5 K may be due to several different effects, such as the presence of low-lying states with  $S < 8$ , zero-field splitting, and/or intermolecular antiferromagnetic interactions. All these factors are expected to determine variations of the magnetization curves from simple Brillouin behavior.<sup>26</sup>

- (21) Armstrong, W. H.; Roth, M. E.; Lippard, S. J. *J. Am. Chem. Soc.* **1987**, *109*, 6318.  
 (22) De Paula, J. C.; Beck, W. F.; Brudvig, G. W. *J. Am. Chem. Soc.* **1986**, *108*, 4002.  
 (23) Vincent, J. B.; Christmas, C. A.; Chong, H.-R.; Li, Q.; Boyd, P. D. W.; Huffman, J. C.; Hendrickson, D. N.; Christou, G. *J. Am. Chem. Soc.* **1989**, *111*, 2086.  
 (24) Kurtz, D. M., Jr. *Chem. Rev.* **1990**, *90*, 585.  
 (25) Caneschi, A.; Gatteschi, D.; Laugier, J.; Rey, P.; Sessoli, R.; Zanchini, C. *J. Am. Chem. Soc.* **1988**, *110*, 2795.  
 (26) Carlin, R. L. *Magnetochemistry*; Springer-Verlag: New York, 1986.

The presence of a state with a large spin which is thermally populated at 4.2 K is confirmed by the EPR spectra. Since at least four transitions spaced by ca. 1000 G are observed at high fields, the spin state must be at least  $S = 4$ . The fact that the low-field transitions are more intense than the high-field ones indicates that the sign of  $D$  is negative.<sup>27</sup>

This is the maximum we are able to achieve from a qualitative analysis of the magnetic data. In order to proceed further it is necessary to have an idea of the nature of the low-lying levels. This will be discussed in the following section.

**Model for the Calculations of the Spin Levels.** The total degeneracy of the spin states of eight  $S = 5/2$  spins is 1 679 616, which can be grouped in total spin states  $S$  ranging from 0 to 20. In order to calculate the spin levels, and the magnetic susceptibility, we attempted to use the approach of irreducible tensor operators in order to take full advantage to the total spin symmetry.<sup>16</sup> However, this approach alone is not sufficient to produce tractable matrices for a cluster of this size. For instance the matrices corresponding to  $S = 5$  and  $S = 4$  have dimensions  $n = 16 576$  and 16 429, respectively.

In order to reduce the dimensions of the matrices to be diagonalized, we employed point group symmetry. Tsukerblatt et al.<sup>28</sup> showed that the best way to do that is to use permutation symmetry for the different spin sites of the cluster, because the spin Hamiltonian is symmetric relative to interchange of identical particles. For  $n$  identical particles the permutation group is  $\pi_n$ , which has  $n!$  elements and a number of irreducible representations which can be obtained using the Young tableaux. For instance if we must consider four identical particles, the appropriate group is  $\pi_4$ , which has 24 elements, grouped in five classes corresponding to five irreducible representations of dimensions 1, 1, 2, 3, 3. This means that the highest degeneracy of the total spin levels for four identical particles is 3.

The  $\pi_4$  group is isomorphous to the point group  $T_d$ , which is certainly more familiar to chemists, and the irreducible representations of  $\pi_4$  correspond to the well-known representations  $A_1, A_2, E, T_1$ , and  $T_2$  of  $T_d$ . Therefore it is convenient to use the latter to characterize the symmetry of the spin levels.

In order to assign the appropriate symmetry labels to the total spin functions of four identical particles, it is sufficient to investigate their behavior under the operations of the group  $T_d$ . For instance, for four  $S = 5/2$  the total spin function characterized by  $S = 10$  and  $M_s = 10$  corresponds to  $|^5/2 \ ^5/2 \ ^5/2 \ ^5/2\rangle$ , where the function is written with the  $|m_1 m_2 m_3 m_4\rangle$  components of the four  $S = 5/2$  spins on the individual centers. It is easy to verify that this function remains unaltered for any interchange of two particles; therefore, it is a basis for the totally symmetric irreducible representation of  $T_d$  ( $\pi_4$ ). We may indicate this function as  $^2A_1$ . By writing explicitly the total spin functions, we can classify them as shown in Table I.

In  $Fe_8$  there is no rigorous symmetry; however, the eight iron(III) ions are not far from  $D_2$  symmetry as far as the exchange

- (27) Abragam, A.; Bleaney, B. *Electron Paramagnetic Resonance of Transition Metal Ions*; Clarendon Press: Oxford, U.K., 1970.  
 (28) Tsukerblatt, B. S.; Belinskii, M. I.; Fainzilberg, V. E. *Sov. Chem. Rev.* **1987**, *9*, 339.

**Table II.** Symmetry Classification of the Total Spin States for  $\text{Fe}_8$  in the  $D_2$  Group

$S$	A	$B_1$	$B_2$	$B_3$	tot. deg
20	1				1
19	2	1	2	2	7
18	10	6	6	6	28
17	22	18	22	22	84
16	60	50	50	50	210
15	118	108	118	118	462
14	243	225	224	224	916
13	419	401	420	420	1660
12	717	690	686	686	2779
11	1088	1061	1092	1092	4333
10	1614	1578	1568	1568	6328
9	2174	2138	2184	2184	8680
8	2841	2799	2780	2780	11200
7	3401	3359	3420	3420	13600
6	3927	3885	3854	3854	15520
5	4139	4097	4170	4170	16576
4	4155	4122	4076	4076	16429
3	3704	3671	3750	3750	14875
2	3019	3001	2940	2940	11900
1	1899	1881	1960	1960	7700
0	703	703	630	630	2666

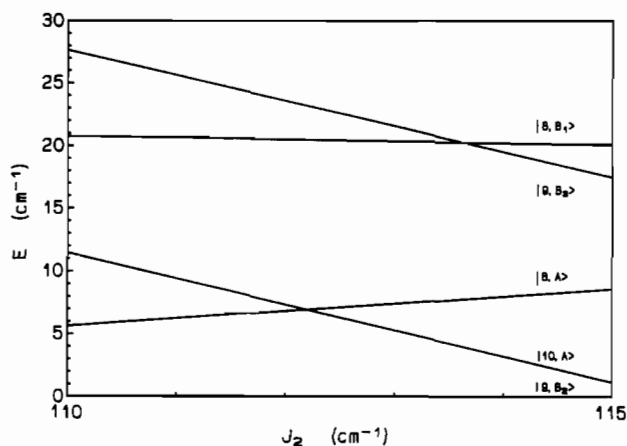
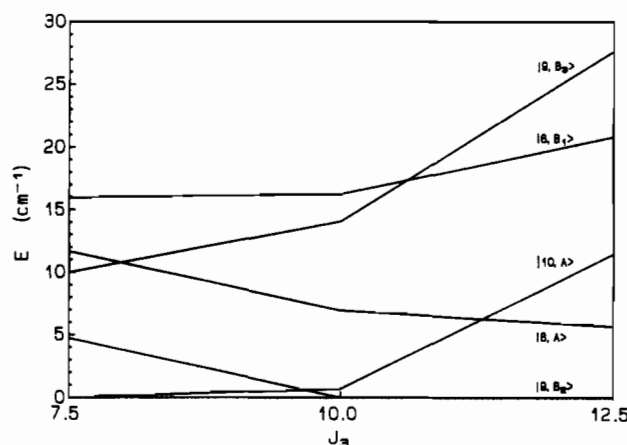
pathways are concerned, as shown in Figures 1 and 5. The eight atoms are divided into two subsets of four, namely 1, 2, 3, and 4 in one set and 5, 6, 7, and 8 in the other. The former couple gives  $S_A = S_1 + S_2 + S_3 + S_4$ , and the latter  $S_B = S_5 + S_6 + S_7 + S_8$ . The symmetry of each subset is also  $D_2$ ; therefore, we can classify the states as shown in Table I. In order to take into account the fact that the point symmetry is  $D_2$  and not  $T_d$ , we have just to use the correlation tables, taking into account the difference between the  $S_A$  and  $S_B$  subsets.

In order to classify the total spin states  $S = S_A + S_B$  we have to write them down explicitly and look at their behavior in the group  $D_2$ . The overall classification schemes appropriate for  $\text{Fe}_8$  is shown in Table II. Actually, since the two subsets of intermediate spin states  $|S_A M_A\rangle$  and  $|S_B M_B\rangle$  do not mix with each other, the irreducible representation  $\Gamma$  of  $|S_A M_A \Gamma_A S_B M_B \Gamma_B S \Gamma\rangle$  is just given by the direct product  $\Gamma_A \otimes \Gamma_B$ . The validity of this approach has been checked on systems of eight  $S = 3/2$  spins, which are tractable without introducing point group symmetry.

By taking advantage of the symmetry, we find that the largest blocks are now  $4170 \times 4170$  compared to  $16\,576 \times 16\,576$  and computation time is also reduced since the number of matrix interactions ( $J_i S_i \cdot S_j$ ) which need to be calculated is reduced by a factor of  $4/13$  for each matrix element.

**Calculation of the Spin Levels.** Notwithstanding the simplifications so far introduced a full calculation for a given set of parameters requires roughly 70 h on our RISC 6000 computer. Therefore we could not afford a random calculation with large variations of the parameters in order to identify the ranges which could reproduce the experimental data. This simply would have been too time consuming. In order to overcome, this problem we made sample calculations in a system with eight  $S = 3/2$  spins. It was hoped that in this way it might be possible to find approximately the ratios between the  $J_i$  values which reproduce analogous magnetic behavior to the  $\text{Fe}_8$  cluster, namely  $\chi T$  increasing on decreasing temperature, reaching a plateau at low temperature corresponding to a high-spin state. We use the correspondence  $S = 10$  for  $\text{Fe}_8$  with  $S = 6$  for the cluster of eight  $S = 3/2$  spins; therefore, we looked for the conditions under which the ground state is larger than 4, and several high-spin states ( $S > 4$ ) are close to it.

Following this procedure we found that, in order to meet these conditions,  $J_4$  must be slightly larger than  $J_3$ , and  $J_1 \approx J_2$ . This marks a difference with the relative values of  $J_1$  and  $J_2$ , which have been used<sup>14,21</sup> for butterfly iron complexes. However if we assume  $J_1 \ll J_2$ , as generally used<sup>14,21</sup> in those cases, a ground  $S = 6$  state is strongly stabilized compared to all the others.

**Figure 6.** Energy of the lowest lying spin states as a function of  $J_2$ .**Figure 7.** Energy of the lowest lying spin states as a function of  $J_3$  ( $J_4 = 2J_3$ ).

Given the structural similarity of the part of the  $\text{Fe}_8$  cluster given by Fe's 1, 2, 3, and 4 to the butterfly complexes, an obvious starting point in fitting the experimental data was to use coupling constants similar to those found in the literature for the  $\text{Fe}_4\text{O}_2$  butterfly complexes and typical values for the hydroxy bridges.<sup>14,24</sup> The  $\chi T$  vs  $T$  curve calculated with  $J_1 = 20 \text{ cm}^{-1}$ ,  $J_2 = 120 \text{ cm}^{-1}$ ,  $J_3 = 15 \text{ cm}^{-1}$ , and  $J_4 = 35 \text{ cm}^{-1}$  is given in Figure 2. All the known iron butterfly compounds have a very large difference between  $J_1$  and  $J_2$  which, in this compound, results in a  $|10, A\rangle$  ground state and a  $|9, B_3\rangle$  first excited state more than  $25 \text{ cm}^{-1}$  higher in energy. This is reflected in Figure 2, where the  $\chi T$  curve goes to  $55 \text{ emu K mol}^{-1}$  at low temperature.

In order to determine the effect of changes in the coupling constants on the ground state and the low-lying energy levels, we have plotted the eigenvalues for a number of states against the coupling coefficients  $J_2$  and  $J_3$ . Figure 6 shows how the eigenvalues of the lowest lying states depend on  $J_2$ . Increasing  $J_2$  stabilizes the  $|10, A\rangle$  and  $|9, B_3\rangle$  states; a similar plot in which both  $J_1$  and  $J_2$  were varied but with  $J_1 - J_2$  kept constant resulted in a set of nearly parallel lines. Hence the difference between  $J_1$  and  $J_2$  is the important parameter here. Therefore Figure 6 suggests that a large difference between  $J_1$  and  $J_2$  will result in an isolated  $|10, A\rangle$  ground state, in accordance with the trends observed in the analogous  $S = 3/2$  calculations. In Figure 7 we give the energy levels of the low-lying states as a function of  $J_3$ , keeping  $J_4 = 2J_3$ . Increasing these parameters destabilizes the  $|10, A\rangle$  state relative to the  $|9, B_2\rangle$  and the  $|8, B_1\rangle$  states.

Better agreement with the experimental data was obtained by increasing  $J_1$  to  $102 \text{ cm}^{-1}$  at which point there are  $|10, A\rangle$  and  $|9, B_2\rangle$  states separated by less than  $0.5 \text{ cm}^{-1}$  and well separated ( $20 \text{ cm}^{-1}$ ) from the other spin states. The agreement between the calculated curve and the experimental data, Figure 2, can be

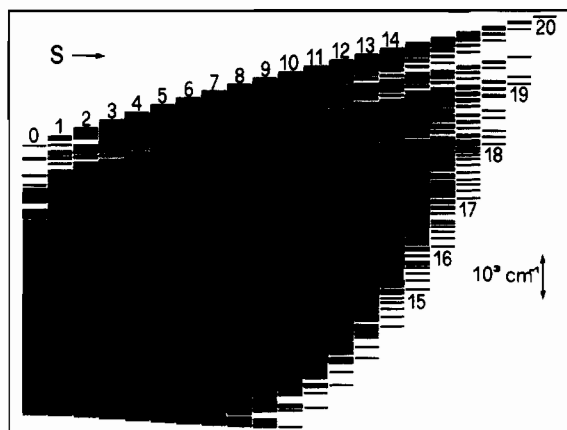


Figure 8. Calculated energy levels for Fe<sub>8</sub>.  $J_1 = 102$ ,  $J_2 = 120$ ,  $J_3 = 15$ , and  $J_4 = 35$  cm<sup>-1</sup>.

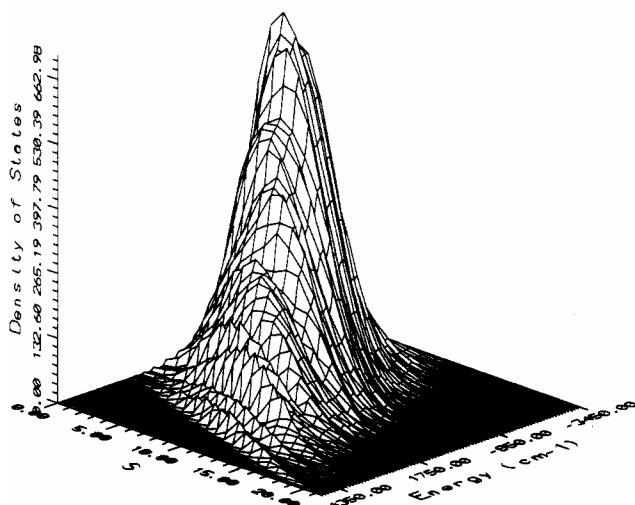


Figure 9. Calculated density of states for Fe<sub>8</sub>. The parameters are the same as in Figure 8. The horizontal axes correspond to the total spin values  $S$  and to the energies.

considered satisfactory given the size of the calculation and the time required.<sup>29</sup>

The  $S = 10$  spin state can be described by a predominant spin configuration in which the spins of the Fe<sub>5</sub>, Fe<sub>6</sub>, Fe<sub>7</sub>, and Fe<sub>8</sub> are parallel to each other, while the spins of Fe<sub>1-4</sub> are alternatively up and down. In fact the spins of Fe<sub>3</sub> and Fe<sub>4</sub> can be set up, and Fe<sub>1</sub> and Fe<sub>2</sub> down. The use of  $J_4 > J_3$  determines the parallel alignment of the spins of the Fe<sub>5-8</sub> ions.

The energies of the spin levels corresponding to the fit are shown in Figure 8. It is apparent that the large number of spin states contained within a maximum of 9000 cm<sup>-1</sup> determines a *quasi-continuum* which corresponds to the structure expected for infinite assemblies of spins. Figure 8 also shows that the high-energy side of the bands is characterized by high-spin states, while close to the bottom only states with  $S \leq 10$  are present. As a consequence, if the susceptibility could be measured in a sufficiently high range of temperature,  $\chi T$  would be seen to decrease initially, go through a minimum, and increase at lower temperature. Figure 9 shows the density of states in a three-dimensional plot from which it is clear that the maximum density is achieved for low-spin states and relatively low energies.

(29) In this range of  $J$  parameters we did not find any evidence of a ground state with  $S < 9$  which could reproduce the experimental data.

In order to justify the apparently large difference between the  $J_1$  value found for this compound and those given in the literature, we have compared the structural details of this compound with those of several other butterfly complexes.<sup>14,20,21</sup> The most consistent difference between the two sets of complexes lies in the Fe–O–Fe angles. For instance the Fe<sub>1</sub>–O–Fe<sub>3</sub> angle is 128.5° and the Fe<sub>3</sub>–O–Fe<sub>2</sub> angle is 127.7°, while the corresponding angles in the butterfly complexes are approximately 120 and 130°, respectively. The corresponding Fe–Fe distances also change with the larger the angle, the greater the distance. With this in mind we have performed some sample calculations on a butterfly complex in which the “wing-body” interactions were allowed to differ. In these calculations  $J_{13} = J_{24} = 135$  cm<sup>-1</sup> and  $J_{12}$  and  $J_{14} = J_{23}$  were allowed to vary, the subscripts refer to the numbering scheme in Figure 5. The calculated susceptibility was compared to published values, and good fits could be obtained in which both  $J_{12}$  and  $J_{14}$  were of a magnitude similar to that of  $J_{13}$ . Hence the small difference between  $J_{13}$  and  $J_{14}$  was sufficient to allow  $J_{12}$  to have a much larger value. Although this model may be more appealing than that used by Hendrickson et al.<sup>14</sup> due to the closer magnetic structural correlation, it introduces a third parameter into a system which can already be well described by a two-parameter model. However, the two parameters which were varied,  $J_{12}$  and  $J_{14}$ , were found to be strongly correlated such that the difference between the two parameters is the better defined parameter. The large “body–body” interaction,  $J_{12}$ , found in these analyses is consistent with that which was found to reproduce the experimental data for the Fe<sub>8</sub> cluster.

## Conclusions

In the field of iron clusters Fe<sub>8</sub> is the one with the highest spin in the ground state so far reported. The high-spin multiplicity is determined by the combined effects of antiferromagnetic coupling constants and the complex exchange topology of the cluster, which allows large spin frustration effects. In this respect Fe<sub>8</sub> is similar to the Mn<sub>12</sub><sup>19,30</sup> and Mn<sub>6</sub>(NITPh)<sub>6</sub><sup>25</sup> complexes, which also have been reported to have high-spin multiplicities in the ground state as a result of antiferromagnetic coupling. Fe<sub>8</sub>, like Mn<sub>6</sub>(NITPh)<sub>6</sub>, does not show any anomaly in the ac susceptibility like the one observed in Mn<sub>12</sub>, where frequency-dependent relaxation effects were reported.<sup>19</sup> The main difference between the two types of compounds lies in the magnetic anisotropy, which is much larger in Mn<sub>12</sub> compared to the other two. Therefore, it may be concluded that the superparamagnetic-like behavior of Mn<sub>12</sub> must be associated with large magnetic anisotropy effects.

The other iron(III) clusters reported so far have been found generally to have low-spin ground states ( $S = 0, 1/2$ ), and only in some Fe<sub>6</sub> clusters spin frustration effects were found to yield a ground  $S = 5$  state.<sup>4</sup> With the present compound the conditions which are required in order to have a high-spin ground state become better defined.

**Acknowledgment.** Thanks are due to Doctor Maurice Guillot of the Service National des Champs Intenses of the CNRS-Grenoble, for performing the high magnetic field magnetization measurements. The financial support of the MURST and CNR, Progetto Finalizzato Materiali Speciali per Tecnologie Avanzate, is gratefully acknowledged.

(30) Boyd, P. D. W.; Li, Q.; Vincent, J. B.; Folting, K.; Chang, H.-R.; Streib, W. E.; Huffman, W. E.; Christou, J. C.; Hendrickson, D. N. *J. Am. Chem. Soc.* **1988**, *110*, 8537.